Resonance Raman Spectra of the Nitric Oxide Adducts of Ferrous Cytochrome P450cam in the Presence of Various Substrates

Songzhou Hu and James R. Kincaid*

Contribution from the Chemistry Department, Marquette University, Milwaukee, Wisconsin 53233. *Received April 9, 1991*

Abstract: Resonance Raman spectra of the nitric oxide adducts of ferrous cytochrome P450cam (from *Pseudomonas putida*) in the adamantanone-, camphor-, and norcamphor-bound forms, as well as in the substrate-free form, are reported. The lowered frequency of the ν_4 (1372 cm^{-1}) and ν_3 (1499 cm^{-1}) modes is consistent with the presence of endogenous thiolate ligation. The three expected normal modes of the natural abundance nitric oxide adduct of ferrous cytochrome P450cam are detected at 1591, 554, and 446 cm^{-1} and are assigned to ν(N–O), $\nu(Fe^{II}–NO)$, and $\delta(Fe^{II}–NO)$, respectively, based on a normal mode analysis, although extensive mixing of the latter two modes is indicated. The very strong band at 554 cm^{-1} shifts to 539 ($^{15}N^{16}O$), 552 ($^{14}N^{18}O$), and 538 cm^{-1} ($^{15}N^{18}O$) as the mass of NO increases incrementally by one atomic unit, while the 446-cm^{-1} feature exhibits a monotonous downshift to 442 ($^{15}N^{16}O$), 440 ($^{14}N^{18}O$), and 437 cm^{-1} ($^{15}N^{18}O$). The substrate sensitivity of these two bands, distinctly different from those observed for the intrinsically linear Fe^{II}–CO (Uno, T., et al. *J. Biol. Chem.* **1985**, *260*, 2023–2026) and Fe^{III}–NO (Hu, S.; Kincaid, J. *J. Am. Chem. Soc.* **1991**, *113*, 2843–2850) adducts, is discussed in relation to the enzyme–catalyzed regio- and stereospecific hydroxylation of camphor.

Introduction

Cytochrome P450cam, the terminal oxidase in the *d*-camphor hydroxylase system of the bacterium *Pseudomonas putida*, catalyzes the regio- and stereospecific hydroxylation of its substrate, camphor, at the 5-exo position.[1] This enzyme has been the most systematically investigated member among a group of b-type heme proteins that gives rise to split Soret bands in the reduced carbon monoxide bound state, with the low-energy component being observed at 450 nm.[2] The molecular structure of P450cam has been well established by numerous spectroscopic studies[3] and more recently by X-ray crystal structural determination.[4] Unlike other heme proteins, such as myoglobin and hemoglobin, cytochrome P450cam utilizes the thiolate of cys-357 as the proximal ligand of the heme iron atom and possesses a nonpolar environment on the distal side of the heme plane. In the substrate-free form, a network of hydrogen-bonded water molecules occupies the substrate pocket and a hydroxide ion or water serves as a distal-side axial ligand,[4b] giving rise to a low-spin ferric heme iron. Upon the binding of camphor, solvent molecules are expelled from the active site to form a pentacoordinated,[4a] high-spin heme iron. The substrate is held above the heme distal surface by a hydrogen-bonding interaction between the carbonyl oxygen and the side chain hydroxyl group of Tyr-96, in addition to a lock-and-key hydrophobic contact between its *gem*-dimethyl groups (C-8 and C-9) and Leu 244.

The catalytic cycle of cytochrome P450cam includes four spectrally discernable states: a low-spin substrate-free ferric form, a high-spin camphor-bound ferric state, a camphor-bound ferrous state, and a low-spin ternary adduct of dioxygen–camphor–ferrous enzyme. An interesting aspect of the cytochrome P450 chemistry is the substrate dependence of reactivity and physical properties. For example, the binding of substrate camphor lifts the midpoint potential of the ferric heme iron from −300 to −173 mV, converts the spin state from low spin to high spin,[5] lowers the ligand affinity of ferrous heme iron for carbon monoxide by 20-fold,[6] and greatly stabilizes the quasistable oxygenated intermediate.[7] Furthermore, the enzyme metabolizes the substrate and its analogues with different regio- and stereospecificity.[8] Thus, it is of particular interest to understand the role the substrate plays in controlling the enzymatic reactions at various stages.

Previously, we investigated the resonance Raman (RR) spectra of the nitric oxide adducts of ferric cytochrome P450cam to assess the interaction of substrates with the bound ligand.[9] The results, along with those of a RR study of the carbon monoxide adduct of the ferrous cytochrome P450cam[10] and a NMR characterization of the cyanide adduct of the ferric enzyme,[11] suggest that the bound substrate perturbs the intrinsically linear Fe–XY linkage.

(1) Gunsalus, I. C.; Meeks, J. R.; Lipscomb, J. D.; Debrunner, P.; Münck, E. In *Molecular Mechanism of Oxygen Activation*; Hayaishi, O., Ed.; Academic Press: New York, 1974, pp 559–613.

(2) (a) Sato, R.; Omura, T., Eds. *Cytochrome P450*; Academic Press: New York, 1978. (b) Ortiz de Montellano, P. R., Ed. *Cytochrome P450 Structure, Mechanism, and Biochemistry*; Plenum Press: New York, 1986. (c) Schuster, I., Ed. *Cytochrome P450: Biochemistry and Biophysics*; Traylor & Francis: Bristol, PA, 1989.

(3) (a) Guengerich, F. P.; McDonald, T. L. *Acc. Chem. Res.* **1984**, *17*, 9–16. (b) Sligar, S. G.; Gelb, M. H.; Heimbrook, D. C. *Xenobiotica* **1984**, *14*, 63–86. (c) Murray, R. I.; Fisher, M. T.; Debrunner, G.; Sligar, S. G. In *Metalloproteins Part I: Metal Proteins with Redox Roles*; Harrison, P. M., Ed.; Verlag Chemie: Weinheim, 1985; p 157. (d) Dawson, J. H.; Eble, K. S. *Adv. Inorg. Bioinorg. Mech.* **1986**, *4*, 1–64. (e) Black, S. D.; Coon, M. J. *Adv. Enzymol. Relat. Areas Mol. Biol.* **1987**, *60*, 35–87. (f) Dawson, J. H.; Sono, M. *Chem. Rev.* **1987**, *87*, 1255–1276. (g) Dawson, J. H. *Science* **1988**, *240*, 433–439.

(4) (a) Poulos, T. L.; Finzel, B. C.; Gunsalus, I. C.; Wagner, G. C.; Kraut, J. *J. Biol. Chem.* **1985**, *260*, 16122–16130. (b) Poulos, T. L.; Finzel, B. C.; Howard, A. J. *Biochemistry* **1986**, *25*, 5314. (c) Poulos, T. L.; Finzel, B. C.; Howard, A. J. *J. Mol. Biol.* **1987**, *195*, 687–700. (d) Poulos, T. L.; Howard, A. J. *Biochemistry* **1987**, *26*, 8165–8174. (e) Raag, R.; Poulos, T. L. *Biochemistry* **1989**, *28*, 917–922. (f) Raag, R.; Poulos, T. L. *Biochemistry* **1989**, *28*, 7586–7592. (g) Raag, R.; Swanson, B. A.; Poulos, T. L.; Ortiz de Montellano, P. R. *Biochemistry* **1990**, *29*, 8119–8126. (h) Raag, R.; Poulos, T. L. *Biochemistry* **1991**, *30*, 2674–2684.

(5) (a) Sligar, S. G. *Biochemistry* **1976**, *15*, 5399–5406. (b) Sligar, S. G.; Gunsalus, I. C. *Proc. Natl. Acad. Sci. U.S.A.* **1976**, *73*, 1078–1082. (c) Fisher, M. T.; Sligar, S. G. *J. Am. Chem. Soc.* **1985**, *107*, 5108.

(6) Peterson, J. A.; Griffin, B. W. *Arch. Biochem. Biophys.* **1972**, *151*, 427–433.

(7) (a) Ishimura, Y.; Ullrich, V.; Peterson, J. A. *Biochem. Biophys. Res. Commun.* **1971**, *42*, 147–153. (b) Lipscomb, J. D.; Sligar, S. G.; Namtvedt, M. J.; Gunsalus, I. C. *J. Biol. Chem.* **1976**, *251*, 1116–1124. (c) Debey, P.; Balny, C.; Douzou, P. *FEBS Lett.* **1976**, *69*, 231–235, 236–239. (d) Eisenstein, L.; Debey, P.; Douzou, P. *Biochem. Biophys. Res. Commun.* **1977**, *77*, 1377–1383.

(8) (a) Gelb, M. H.; Heimbrook, D. C.; Malkonen, P.; Sligar, S. G. *Biochemistry* **1982**, *21*, 370–377. (b) White, R. E.; McCarthy, M.-B.; Edeberg, K. D.; Sligar, S. G. *Arch. Biochem. Biophys.* **1984**, *228*, 493–502. (c) Eble, K. S.; Dawson, J. H. *J. Biol. Chem.* **1984**, *259*, 14389–14393. (d) Atkins, W. A.; Sligar, S. *J. Am. Chem. Soc.* **1987**, *109*, 3754–3760. (e) Atkins, W. A.; Sligar, S. *Biochemistry* **1988**, *27*, 1610–1616. (f) Atkins, W. A.; Sligar, S. G. *J. Biol. Chem.* **1988**, *263*, 18842–18849.

(9) Hu, S.; Kincaid, J. R. *J. Am. Chem. Soc.* **1991**, *113*, 2843–2850.

(10) (a) Uno, T.; Nishimura, Y.; Makino, R.; Iizuka, T.; Ishimura, Y.; Tsuboi, M. *J. Biol. Chem.* **1985**, *260*, 2023–2026. (b) Tsuboi, M. *Indian J. Pure Appl. Phys.* **1988**, *26*, 188–191.

(11) Shiro, Y.; Iizuka, T.; Makino, R.; Ishimura, Y.; Morishima, I. *J. Am. Chem. Soc.* **1989**, *111*, 7707–7711.

0002-7863/91/1513-9760$02.50/0

In this work, we apply the RR spectroscopy to study the nitric oxide adducts of ferrous cytochrome P450cam, in the adamantanone-bound, camphor-bound, norcamphor-bound, and substrate-free forms, in an effort to characterize the interaction of the bound dioxygen with substrate. The studies are clearly relevant to the physiological reaction inasmuch as the NO adducts of ferrous heme proteins[12] bear the same geometry as that of the dioxygen adducts.[13] By using four isotopic nitric oxide molecules, we are able to observe, for the first time, two isotope-sensitive lines in the low-frequency RR spectra of the NO adducts of ferrous cytochrome P450cam, one showing a zigzag isotope-shifting pattern and the other exhibiting a monotonous downshift as the mass of the isotopic NO molecule increases. The substrate sensitivity of these two lines suggests that only camphor, or an analogue of greater steric bulk (such as adamantanone), can interact with the bound NO.

Materials and Methods

Cytochrome P450cam was isolated and purified from the cell paste of *P. putida*, grown on *d*-camphor as the sole carbon source, according to a modification of the method first described by Gunsalus and Wagner.[14] The highly purified preparation was obtained as the camphor-bound form having a Rz value (absorbance at 391 nm/absorbance at 280 nm) greater than 1.50. The substrate-free form of the enzyme was prepared by a passage of the camphor-bound enzyme over a Sephadex G-25 column, which was previously equilibrated with 50 mM MOPS buffer (pH = 7.4). The norcamphor-bound form was formed by proper dilution of a 10 mM stock solution of norcamphor into the substrate-free enzyme solution. The adamantanone-bound cytochrome P450cam was prepared by saturating the substrate-free preparation with solid adamantanone, and the excess was removed by centrifugation.

$Na^{15}NO_2$ (99.5%) was purchased from MSD. The ^{18}O-labeled nitrites ($NaN^{18}O_2$ and $Na^{15}N^{18}O_2$) were synthesized from $NaNO_2$ and $Na^{15}NO_2$ by acid-catalyzed oxygen atom exchange in bulk solvent $H_2{}^{18}O$ (99.5%, MSD).[15] The isotopic enrichment was checked by monitoring the Raman spectral feature (413.1-mm excitation) of natural abundance nitrite at 1331 cm^{-1}, which shifts to 1308 cm^{-1} ($Na^{15}N^{16}O_2$), 1300 cm^{-1} ($Na^{14}N^{18}O_2$) and 1276 cm^{-1} ($Na^{15}N^{18}O_2$).

The preparation of the nitric oxide adducts of ferrous cytochrome P450cam in various substrate-bound forms, as well as those of ferrous myoglobin and hemoglobin, was performed by anaerobic decomposition of properly isotope-labeled sodium nitrite with dithionite. Specifically, about 0.2 mL of heme protein solution was placed in a 5 mm NMR tube. After the tube was sealed with a rubber septum, it was vigorously degassed by flushing nitrogen for several minutes. The heme protein was then reduced by injecting about 50-fold excess aqueous solution of sodium dithionite, followed by 20-fold sodium nitrite to form the nitric oxide adduct.

Resonance Raman spectra were acquired on a Spex Model 1403 system equipped with a Spex DM1B data station and a Hamamatsu R-928 photomultiplier. Excitation lines were from Coherent Innova Model 100-K3 Kr^+ ion (406.7 and 413.1 nm), Liconix Model 4240NB helium:cadmium (441.6 nm), and Spectra-Physics 2025-05 Ar^+ ion lasers (lines between 457.9 and 514.5 nm). The laser power was kept between 10-15 mw at the sample. For the measurement of the nitric oxide adducts of cytochrome P450cam, the NMR tube was positioned in a double-walled glass cell of in-house design using backscattering geometry. Throughout the spectral acquisition, the NMR tube was kept spinning and the temperature was maintained at 0 °C by flushing with prechilled dry nitrogen.

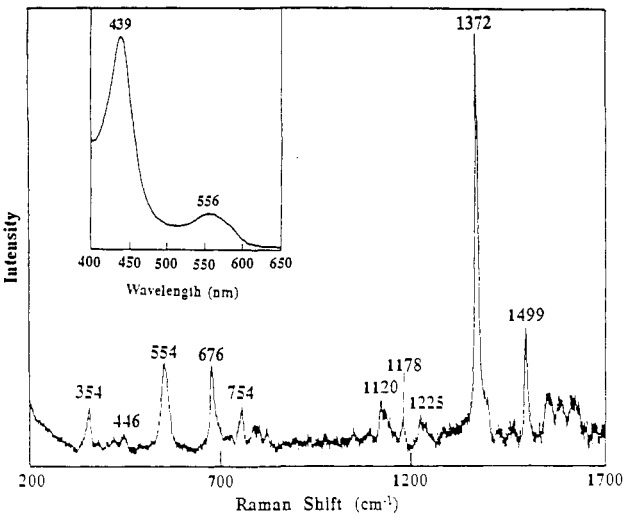

Figure 1. Overall resonance Raman spectrum (413.1-nm excitation) of the natural abundance nitric oxide adduct of ferrous cytochrome P450cam in the presence of saturated adamantanone. The concentration of the protein was approximately 100 μM in 50 mM MOPS buffer at pH 7.4.

Results and Discussion

A. High-Frequency RR Spectrum and Detection of the ν(N–O) Mode. Anaerobic reduction of ferric cytochrome P450cam with dithionite in the presence of nitrite or exposure of ferrous enzyme to nitric oxide yields a spectrally distinct species,[16] exhibiting a Soret absorption band maximum at 439 nm as shown in the inset of Figure 1. The considerably red-shifted wavelength of the Soret peak, relative to that observed for the nitrosyl adduct of myoglobin, reflects the presence of the endogenous thiolate ligand.

Figure 1 displays the RR spectrum of the natural abundance NO adduct of adamantanone-bound cytochrome P450cam obtained with excitation at 413.1 nm. The sample integrity was checked by measuring the electronic absorption spectrum before and after laser illumination and by recording the RR spectrum in the ν_4 region regularly to monitor the possible formation of photodissociated products. As shown in Figure 1, no trace of a feature at 1341 cm^{-1} (the frequency of the ν_4 mode of ferrous cytochrome P450cam[17]) is detected, thus proving that the RR spectrum displayed is not contaminated with photoproducts. Although the spectrum between 1300 and 1700 cm^{-1} is typical for a six-coordinated, low-spin adduct of a π-acid ligand, the spectral pattern is substantially altered compared to that of the nitric oxide adduct of myoglobin and horseradish peroxidase.[18] The frequencies of the ν_4 and ν_3 modes are lowered and the intensity of ν_3 is enhanced. Furthermore, the reduction of the ferric nitric oxide adduct of cytochrome P450cam is accompanied by a 3-cm^{-1} downshift of ν_4. In contrast, the ν_4 is unchanged upon the reduction of the corresponding myoglobin and peroxidase derivatives.

The high-frequency RR spectra of heme proteins exhibit reliable "marker bands", which can be used to monitor the oxidation and spin states of heme iron.[19] The most prominent feature observed in the Soret-excited spectrum, ν_4, is described as an in-plane symmetric stretching mode of the porphyrin skeleton and is termed the oxidation state marker band.[20] It occurs at about 1370 cm^{-1}

(12) (a) Deatherage, J. F.; Maffat, K. *J. Mol. Biol.* **1979**, *134*, 401–417. (b) Piciulo, P. L.; Rupprecht, G.; Scheidt, W. R. *J. Am. Chem. Soc.* **1974**, *96*, 5293–5295. (c) Scheidt, W. R.; Frisse, M. E. *J. Am. Chem. Soc.* **1975**, *97*, 17–21. (d) Scheidt, W. R.; Piciulo, P. L. *J. Am. Chem. Soc.* **1976**, *98*, 1913–1919. (e) Scheidt, W. R.; Brinegar, A. C.; Ferro, E. B.; Kirner, J. F. *J. Am. Chem. Soc.* **1977**, *99*, 7315–7322.

(13) (a) Collman, J. P.; Gagne, R. R.; Reed, C. A.; Robinson, W. T.; Rdiley, G. A. *Proc. Natl. Acad. Sci. U.S.A.* **1974**, *71*, 1326–1329. (b) Jameson, G. B.; Rodley, G. A.; Robinson, W. T.; Gagne, R. R.; Reed, C. A.; Collman, J. P. *Inorg. Chem.* **1978**, *17*, 850–857. (c) Jameson, G. B.; Molinaro, F. S.; Ibers, J. A.; Collman, J. P.; Brauman, J. I.; Rose, E.; Suslick, K. S. *J. Am. Chem. Soc.* **1980**, *102*, 3224. (d) Philips, S. E. V. *J. Mol. Biol.* **1980**, *142*, 531–554. (e) Shaanan, B. *Nature* **1982**, *296*, 683–684.

(14) Gunsalus, I. C.; Wagner, G. C. *Methods Enzymol.* **1978**, *52*, 166–188.

(15) (a) Van Etten, R. L.; Risley, J. M. *J. Am. Chem. Soc.* **1981**, *103*, 5633–5636. (b) Rajenden, C.; Van Etten, R. L. *Inorg. Chem.* **1986**, *25*, 876–978.

(16) O'Keeffe, D. H.; Ebel, R. E.; Peterson, J. A. *J. Biol. Chem.* **1978**, *253*, 3509–3516.

(17) (a) Ozaki, Y.; Kitagawa, T.; Kyogoku, Y.; Shimada, H.; Iizuka, T.; Ishimura, Y. *J. Biochem.* **1976**, *80*, 1447–1457. (b) Champion, P. M.; Gunsalus, I. C.; Wagner, G. C. *J. Am. Chem. Soc.* **1978**, *100*, 3743–3751. (c) Bangchaoenpaurpong, O.; Champion, P. M.; Martinis, S. A.; Sligar, S. G. *J. Chem. Phys.* **1987**, *87*, 4273–4284.

(18) Benko, B.; Yu, N.-T. *Proc. Natl. Acad. Sci. U.S.A.* **1983**, *80*, 7042–7046.

(19) (a) Yamamoto, T.; Palmer, G.; Gill, D.; Salmeen, I. T.; Rimai, L. *J. Biol. Chem.* **1973**, *248*, 5211. (b) Spiro, T. G.; Strekas, T. C. *J. Am. Chem. Soc.* **1974**, *96*, 338.

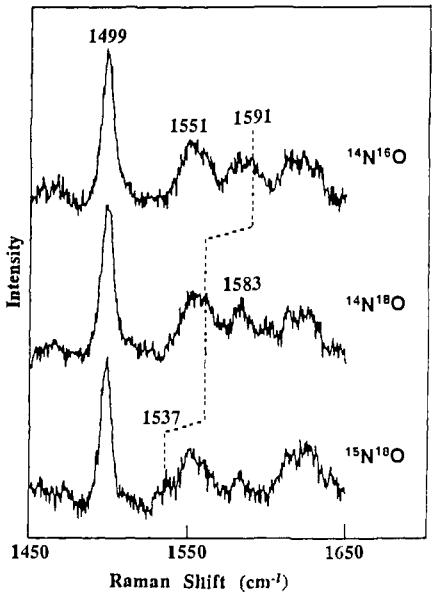

Figure 2. Isotopic effect on the resonance Raman spectra (413.1-nm excitation) of the nitric oxide adducts of adamantanone-bound cytochrome P450cam in the ν(N–O) region.

for ferric heme proteins and shifts to about 1355 cm^{-1} upon reduction to the ferrous form. In addition, this mode has also been shown to be particularly sensitive to the electron density of the porphyrin π^* orbitals.[21] For this reason, the ν_4 mode is also referred to as a π electron density marker band.[22] It is expected that the ν_4 frequency will be decreased when more electrons are transferred to the antibonding π^* orbital. For ferrous cytochromes P450 from various sources,[17,23] the ν_4 occurs at an anomalously low frequency ($\sim$1340 cm^{-1}) compared to those of heme proteins possessing a histidyl proximal ligand ($\sim$1355 cm^{-1}). The lowered ν_4 frequency has also been observed for the ferric form, ferrous monoxide adduct,[10] ferric nitric oxide adduct,[9] and the oxygenated intermediate[24] of cytochrome P450cam, although the magnitude is small, owing to the competition for the π electron between the heme and the axial π-acid ligands.

One of the spin state marker bands, ν_3, is also easily identified in the 413.1-nm excited RR spectrum as shown in Figure 1. The frequency of this mode has been shown to be inversely proportional to the core size (Ct–N), i.e., the distance between the porphyrin ring center and pyrrole nitrogen atom.[25] On the basis of the empirical relationship $\nu = K(A - d)$ and the tabulated K (423.7 cm^{-1}/Å) and A (5.53 Å) values for the ν_3 mode,[25d] it is possible

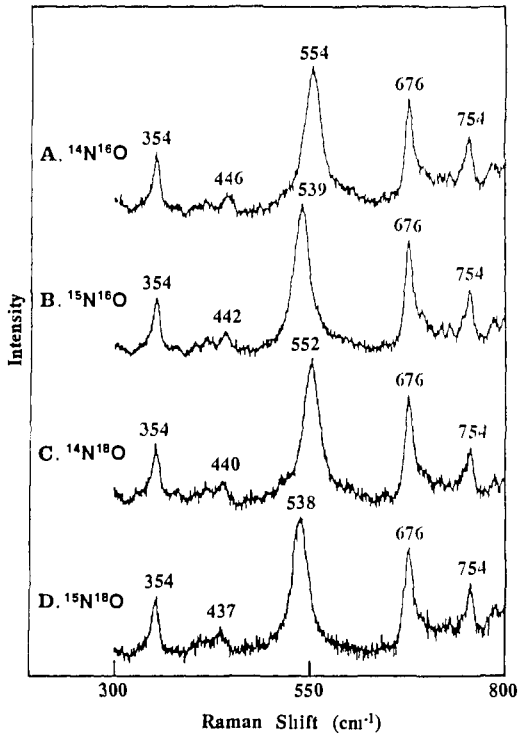

Figure 3. Low-frequency resonance Raman spectra (413.1-nm excitation) of the isotopomeric nitric oxide adducts of adamantanone-bound ferrous cytochrome P450cam.

to estimate the core size from the observed frequency. The result indicates a nearly identical core size (1.98 Å) for the nitric oxide adduct of ferrous myoglobin (ν_3 = 1503 cm^{-1}) and ferric cytochrome P450cam (ν_3 = 1505 cm^{-1}) but a slightly expanded one (1.99 Å) for that of ferrous cytochrome P450cam (ν_3 = 1499 cm^{-1}). Clearly, the effect of thiolate ligation to heme iron in cytochrome P450cam is reflected by both the π electron density of the porphyrin ring and the heme core size.

Figure 2 presents the expanded RR spectrum of the NO adduct of cytochrome P450cam in the presence of adamantanone, along with the $^{14}N^{18}O$ and $^{15}N^{18}O$ isotopomers, in the region where ν(N–O) is likely to occur. A weak feature observed at 1591 cm^{-1} in trace A shifts to 1537 cm^{-1} upon $^{14}N^{16}O/^{15}N^{18}O$ substitution, the expected 54-cm^{-1} downshift confirming its assignment to the ν(N–O). Although this mode is not clearly discernable for the $^{15}N^{16}O$ (spectrum not shown) and $^{14}N^{18}O$ adducts (trace B), owing to the overlap with adjacent heme modes, a slight increase in intensity at 1560 cm^{-1} is apparent. We note that the observed frequency of the ν(N–O) for cytochrome P450cam is substantially lower than that detected for ferrous myoglobin and hemoglobin (at about 1620 cm^{-1}).[26] Similar lowering of the internal stretching frequency of the bound X–Y ligand was also observed for the CO[27] and O_2 adducts[24,28] of cytochrome P450cam, reflecting the presence of the strong electron-donating axial ligand, mercaptide.

B. RR Detection and Assignments of the Normal Modes of the Fe^{II}–NO Fragment in the Nitric Oxide Adduct of Ferrous Cytochrome P450cam. Figure 3 presents the low-frequency RR spectra (excited at 413.1 nm) of the nitric oxide adducts of adamantanone-bound ferrous cytochrome P450cam with $^{14}N^{16}O$, $^{15}N^{16}O$, $^{14}N^{18}O$, and $^{15}N^{18}O$ isotopomers. The spectra are arranged in the order of increasing mass of the NO and the major peaks are labeled. The bands at 354, 676, and 754 cm^{-1} are assigned to the ν_8, ν_7, and ν_{15} modes of the heme skeleton, respectively, according to the nomenclature of Abe and Kitagawa.[20a,b] The remaining

(20) (a) Abe, M.; Kitagawa, T.; Kyogoku, Y. *J. Chem. Phys.* **1978**, *69*, 4526. (b) Kitagawa, T.; Abe, M.; Ogoshi, H. *J. Chem. Phys.* **1978**, *69*, 4516. (c) Li, X. Y.; Czernuszewicz, R. S.; Kincaid, J. R.; Su, Y. O.; Spiro, T. G. *J. Phys. Chem.* **1990**, *94*, 31–46. (d) Li, X. Y.; Czernuszewicz, R. S.; Kincaid, J. R.; Stein, P.; Spiro, T. G. *J. Phys. Chem.* **1990**, *94*, 47–61.

(21) Choi, S.; Spiro, T. G.; Langry, K. C.; Smith, K. M.; Budd, L. D.; LaMar, G. N. *J. Am. Chem. Soc.* **1982**, *104*, 4345–4351.

(22) Spiro, T. G.; Li, X.-Y. In *Biological Applications of Raman Spectroscopy*; Spiro, T. G., Ed.; Wiley: New York, 1988; Vol. III, pp 1–37.

(23) (a) Ozaki, Y.; Kitagawa, T.; Kyogoku, Y.; Imai, Y.; Hashimoto-Yutsudo, C.; Sato, R. *Biochemistry* **1978**, *17*, 5826–5831. (b) Shimizu, T.; Kitagawa, T.; Mitani, F.; Iizuka, T.; Ishimura, Y. *Biochim. Biophys. Acta* **1981**, *670*, 236–242. (c) Tsubaki, M.; Hiwatashi, A.; Ichikawa, Y. *Biochemistry* **1987**, *26*, 4535–4540. (d) Kelly, K.; Rospendowski, B. N.; Smith, W. E.; Wolf, C. R. *FEBS Lett.* **1987**, *222*, 120–124. (e) Hildebrandt, P.; Garda, H.; Stier, A.; Stockburger, M.; Van Dyke, R. A. *FEBS Lett.* **1988**, *237*, 15–20. (f) Anzenbacher, P.; Evangelista-Kirp, R.; Schenkman, J.; Spiro, T. G. *Inorg. Chem.* **1989**, *28*, 4491–4495. (g) Hildebrandt, P.; Greinert, R.; Stier, A.; Taniguchi, H. *Eur. J. Biochem.* **1989**, *186*, 291–302. (h) Hildebrandt, P.; Garda, H.; Stier, A.; Bachmanova, G. I.; Kanaeva, I. P.; Archakov, A. I. *Eur. J. Biochem.* **1989**, *186*, 383–388.

(24) Hu, S.; Schneider, A. J.; Kincaid, J. R. *J. Am. Chem. Soc.* **1991**, *113*, 4815–4822.

(25) (a) Spaulding, L. D.; Cheng, C. C.; Yu, N.-T.; Felton, R. H. *J. Am. Chem. Soc.* **1975**, *97*, 2517. (b) Huang, P. V.; Pommier, J. C. *Acad. Sci. Ser.* **1977**, *C285*, 519. (c) Choi, S.; Lee, J. J.; Wei, Y. H.; Spiro, T. G. *J. Am. Chem. Soc.* **1983**, *105*, 3692–3707. (d) Parthasarathi, N.; Hanson, C.; Yamaguchi, S.; Spiro, T. G. *J. Am. Chem. Soc.* **1987**, *109*, 3865.

(26) (a) Tsubaki, M.; Yu, N.-T. *Biochemistry* **1982**, *21*, 1140–1144. (b) Maxwell, J. C.; Caughey, W. S. *Biochemistry* **1976**, *15*, 388–396.

(27) O'Keefe, D. H.; Eble, R. E.; Peterson, J. A.; Maxwell, J. C.; Caughey, W. S. *Biochemistry* **1978**, *17*, 5845–5852.

(28) Bangchaoenpaurpong, O.; Rizos, A. K.; Champion, P. M.; Jollie, D.; Sligar, S. *J. Biol. Chem.* **1986**, *261*, 8089–8092.

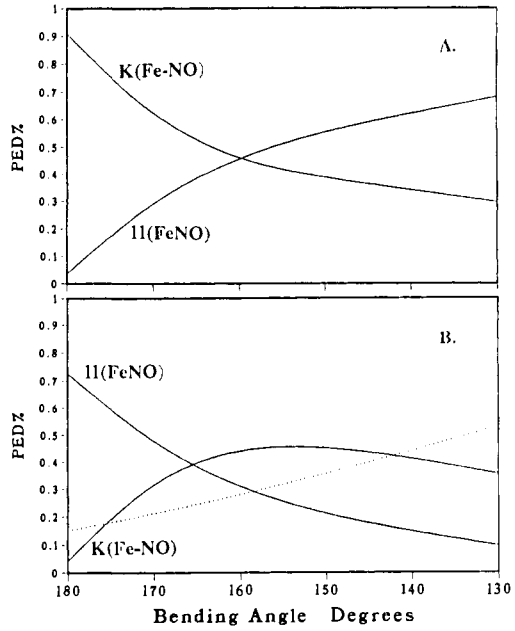

Figure 4. Normal mode composition of the Fe–NO vibrations as a function of the Fe–N–O angle. The upper and lower diagrams are for those of the 522- and 548-cm^{-1} modes of a linear L–Fe–N–O model, respectively. The calculated frequency of both vibrational modes and the force constants used are given in ref 9. The dotted line in the lower diagram represents the contribution from K(Fe–L).

two bands, located at 554 and 446 cm^{-1}, are clearly associated with the bound NO as they show isotope sensitivity. The very strong 554-cm^{-1} feature shifts to 539 ($^{15}N^{16}O$), 552 ($^{14}N^{18}O$), and 538 cm^{-1} ($^{15}N^{18}O$) as the mass of NO increases by one unit. This zigzag isotope-shifting pattern is identical to that observed for the 554-cm^{-1} line in the RR spectrum of ferrous nitrosyl myoglobin[26a] and the 558-cm^{-1} mode of the NO adduct of sulfite reductase.[29] Although no other isotope-sensitive line has been observed previously in the low-frequency RR spectrum of any other ferrous nitrosyl heme protein, we were able to detect another one at 446 cm^{-1} which shows a monotonous downshift to 442 ($^{15}N^{16}O$), 440 ($^{14}N^{18}O$), and 437 cm^{-1} ($^{15}N^{18}O$). While this band is relatively weak, it can still be clearly identified, owing to the simplicity of the spectrum.

Chottard and Mansuy[30] first detected a weak feature in the RR spectrum (excited at 514 nm) of ferrous nitrosyl hemoglobin at 549 cm^{-1}, which shifted to 539 cm^{-1} upon $^{14}N^{16}O$ to $^{15}N^{16}O$ substitution, and assigned it to the stretching mode of the Fe^{II}–NO unit. However, a similar mode at 554 cm^{-1} was later found to be virtually insensitive to the isotopic replacement of terminal oxygen in a subsequent RR spectroscopic study of ferrous nitrosyl myoglobin carried out by Benko and Yu.[18] On the basis of the observed zigzag isotope-shifting pattern, which is characteristic of the bending mode of linear Fe^{II}–CO and Fe^{III}–NO fragments, they reassigned the 554 cm^{-1} to the Fe^{II}–N–O bending vibration rather than to the Fe^{II}–NO stretching mode. Although a similar line has been invariably resonance enhanced for the nitric oxide adducts of ferrous leghemoglobin,[31] mixed-valence cytochrome c oxidase[32] and sulfite reductase,[29] one of the expected two vibrational modes (stretching and bending) in the low-frequency region, has hot been observed before. Our observation of two isotope-sensitive modes in the low-frequency region should help resolve the dispute and provide a definitive vibrational assignment.

Table I. Calculated and Observed Frequencies of ν(N–O), ν(Fe–NO), and δ(FeNO) Modes of the Fe–N–O Fragment in the Nitric Oxide Adduct of Ferrous Cytochrome P450cam[b,c]

mode	obsd (Δ^a)	calcd (Δ^a)	assignment PED
ν_1	1591 (–, ~30, 54)	1593.0 (30.8, 37.8, 69.8)	96% ν(NO)
ν_2	554 (15, 2, 16)	557.2 (12.2, 4.4, 16.4)	57% ν(Fe–NO), 43% δ(FeNO)
ν_3	446 (4, 6, 9)	441.8 (3.4, 5.2, 8.7)	40% δ(FeNO), 14% δ(Fe–NO), 40% ν(Fe–L)
ν_4	not observed	330.6 (2.1, 6.4, 8.4)	52% δ(Fe–L), 24% ν(Fe–NO), 10% δ(FeNO)

[a] The value indicates the isotopic shift of nitric oxide in the order of $^{15}N^{16}O$, $^{14}N^{18}O$, and $^{15}N^{18}O$. [b] Structural parameters of the L–Fe–N–O linkage: d(Fe–N) = 1.74 Å, d(NO) = 1.10 Å, d(Fe–L) = 2.40 Å, ∠FeNO = 150°, and ∠LFeN = 180°. [c] Force constants used: K(N–O) = 10.75, K(Fe–N) = 2.44 mdyn/Å, K(Fe–L) = 2.40 mdyn/Å, k(L–Fe,Fe–N) = 0.20 mdyn/Å, and k(Fe–N,N–O) = 0.20 mydn/Å, H(Fe–N–O) = 0.66 mdyn·Å/rad², H(L–Fe–N) = 0.35 mdyn·Å/rad², k(Fe–N,Fe–N–O) = 0.11 mdyn/rad.

To aid the assignment of the observed three isotope-sensitive bands of the nitric oxide adduct of adamantanone-bound ferrous cytochrome P450cam, we have carried out a normal coordinate calculation based on a simple four-atom L–Fe–N–O system (L stands for CH_3S with a dynamic mass, 47 amu). The molecular geometry of the FeNO fragment was taken from the X-ray crystallographic data of nitrosyl hemoglobin[12a] and iron porphyrin adducts[12b-e] as used before.[9] The d(Fe–N) and d(N–O) distances are 1.74 and 1.10 Å, respectively. The d(Fe–L), taken from the crystallographic data on the CO adduct of cytochrome P450cam,[4f] is 2.40 Å. The L–Fe–N fragment is assumed to be linear. Previously, we have noted in the vibrational analysis of the linear Fe^{III}–NO system that the ν(Fe–NO) (522 cm^{-1}) and δ(FeNO) (546 cm^{-1}) modes move apart rapidly when the valence angle of the Fe–N–O fragment is allowed to decrease. We wish to further point out that the bending process also changes the composition of these two normal modes. This effect is illustrated in Figure 4, in which the potential energy distribution of the observed ν(Fe–NO) and δ(FeNO) in the linear system is plotted against the bending angle. It is evident that a reversal of the mode composition occurs at an ∠FeNO angle of about 160° but the isotopic shift pattern of these two modes is preserved. This behavior was also calculated in an analysis of the bending mode of carbon monoxide to ferrous heme proteins by Li and Spiro.[34] Thus, it is expected that the 554- and 446-cm^{-1} bands are assigned to the ν(Fe–NO) and δ(FeNO) modes, respectively.

In order to fit the calculated frequencies with the experimental results, it was necessary to adjust the force constants previously used for the Fe^{III}–NO system. The resulting force field along with the observed and the calculated frequencies are summarized in Table I. The substantially smaller K(Fe–NO) for the Fe^{II}–NO system (compared to that of the Fe(III)–NO case) reflects the fact that addition of an electron to the Fe^{III} increases back-bonding, thus weakening the Fe^{II}–NO bond. However, the observed higher ν(Fe–NO) frequency for the Fe^{II}–NO case can be attributed to the kinematic effect of a bent Fe–N–O geometry, which tends to push up ν(Fe–NO). As can be seen in the table, we are able to reproduce the isotopic shift pattern of the two isotope-sensitive bands in the low-frequency region with this simple four-atom model. The potential energy distribution analysis shows that, for the above-mentioned geometry and force constant set, the band at 554 cm^{-1} is predominantly stretching is character, while the other one at 446 cm^{-1} is mainly bending in nature, although substantial mode mixing is evident as is expected for a bent system.[34] This result is also consistent with the conclusion drawn

(29) Han, S.; Madden, J. F.; Siegel, M.; Spiro, T. G. *Biochemistry* **1989**, *28*, 5477–5485.
(30) Chottard, G.; Mansuy, D. *Biochem. Biophys. Res. Commun.* **1977**, *77*, 1333–1338.
(31) Desbois, A.; Lutz, M.; Banerjee, R. *Biochim. Biophys. Acta* **1981**, *671*, 184–192.
(32) Rousseau, D. L.; Singh, S.; Ching, Y.-C.; Sassaroli, M. *J. Biol. Chem.* **1988**, *263*, 5681–5685.
(33) Schachtschneider, J. H.; Mortimer, F. S. *Vibrational Analysis of Polyatomic Molecules*; Technical Reports No 231-61, 1964, Shell Development Co., Emeryville, CA.
(34) Li, X. Y.; Spiro, T. G. *J. Am. Chem. Soc.* **1988**, *110*, 6024–6033.

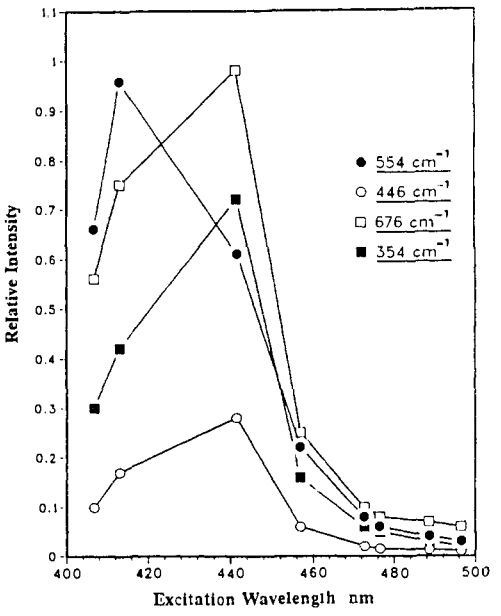

Figure 5. Excitation profile of ν_7 (676 cm^{-1}), ν_8 (354 cm^{-1}), ν(Fe–NO) (554 cm^{-1}), and δ(FeNO) (446 cm^{-1}) modes of the nitric oxide adduct of adamantanone-bound ferrous cytochrome P450cam.

from the qualitative prediction, which is based on the consideration of the kinematic effect of the bending process as discussed above.

We wish to point out here that ν(Fe–NO) and δ(FeNO) exhibit a different enhancement pattern as the excitation line is tuned toward the Soret maximum. Specifically, in the 413.1-nm excited RR spectra, the ν(Fe–NO) mode is stronger than the ν_7 mode and the δ(FeNO) mode is very weak. As the excitation (441.6 nm) was tuned to the proximity of the Soret band (439 nm), the intensity of the ν(Fe–NO) mode becomes weaker and that of the bending mode stronger, relative to the ν_7 mode (e.g., see Figure 8). This prompted us to construct an excitation profile using potassium sulfate and potassium nitrate as internal standards. As shown in Figure 5, the ν(Fe–NO) mode reaches a maximum at 413.1 nm, while the δ(FeNO) mode follows the enhancement pattern of ν_7 and ν_8 heme modes. It is possible that the ν(Fe–NO) mode will maximize at some wavelength between 413 and 440 nm. However, the blue-shifted maximum of the metal–ligand vibrational mode may suggest that its greater enhancement than the corresponding mode in other hemeproteins (e.g., myoglobin and hemoglobin) is a consequence of a contribution from a charge-transfer transition, in addition to the expected π–π^* mechanism.[35]

In the case of the NO adduct of ferric cytochrome P450cam, the effect of proximal cysteinyl ligation was noted to be very strong, as evidenced by the dramatically lowered ν(Fe–NO) frequency. However, this factor seems to be less effective in the case of the NO adduct of ferrous cytochrome P450cam. This stems from the fact that the bending of a linear Fe–N–O linkage substantially increases the energy of the d_{xy}–π^* orbital,[37] thus rendering the transfer of a lone pair on the axial sulfur (p_y) energetically unfavorable. Therefore, it is expected that the difference in ν(Fe–NO) for the Fe^{II}–NO adduct of P450cam and of those proteins possessing a proximal histidyl axial ligand is much smaller than that for the Fe^{III}–NO analogues. In fact, the ν(N–O) (about 1590 cm^{-1}) and ν(Fe–NO) (547 cm^{-1}) of the unperturbed NO adduct of ferrous P450cam (substrate-free form, see Table II) are slightly lower than those observed for the corresponding adduct of ferrous myoglobin (1620 and 555 cm^{-1}, respectively).

C. Low-Frequency RR Spectra of the Nitric Oxide Adducts of Ferrous Myoglobin and Hemoglobin. The observation of two isotope-sensitive bands in the case of cytochrome P450cam prompted us to reinvestigate the RR spectra of ferrous nitrosyl myoglobin and hemoglobin, using the $^{14}N^{16}O$, $^{15}N^{16}O$, $^{14}N^{18}O$, and $^{15}N^{18}O$ isotopomers. The RR spectra of the isotopic derivatives of nitrosyl myoglobin generated by anaerobic decomposition of properly labeled nitrite with dithionite are displayed in Figure 6. In general, these spectra are similar to those reported by Tsubaki and Yu.[26a] The 554-cm^{-1} line is readily observed by its characteristic zigzag isotope-shifting pattern as revealed before. In addition, we also detected a weak feature, located at 449 cm^{-1}, that is sensitive to isotope substitution. It shifts to 447 ($^{15}N^{16}O$), 445 ($^{14}N^{18}O$), and 443 cm^{-1} ($^{15}N^{18}O$). In the spectrum of the natural abundance NO adduct, as shown in trace A of Figure 6, this mode and an adjacent heme mode at 438 cm^{-1} are well resolved, but as the mass of isotopic nitric oxide increases, they coalesce to form a single band of greater intensity. These spectra definitely demonstrate that the 449-cm^{-1} mode, which was previously assigned as a low-frequency heme mode (band VII),[31] is actually associated with the bound nitric oxide.

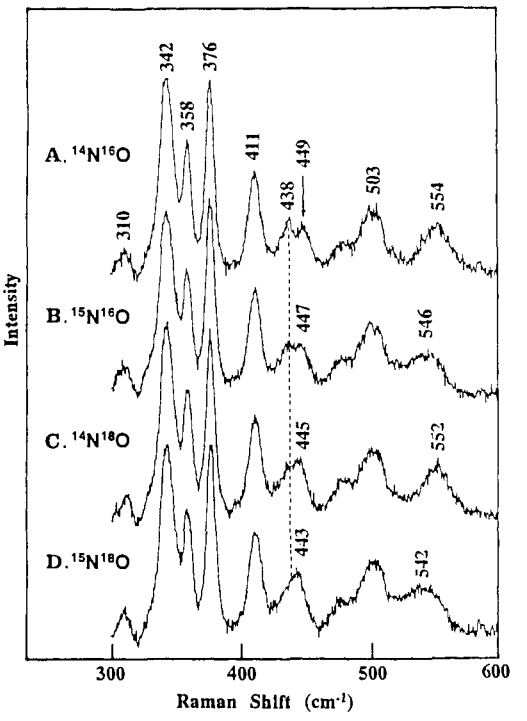

Figure 6. Effect of isotopic substitution on the low-frequency resonance Raman spectra (406.7-nm excitation) of the nitric oxide adduct of ferrous myoglobin. The concentration of myoglobin was 200 μM in 20 mM potassium phosphate buffer at pH 7.0.

Figure 7 shows the low-frequency RR spectra (406.7-nm excitation) of ferrous nitrosyl hemoglobin, formed in the same way as that for myoglobin. The broad feature centered at 430 cm^{-1} in the previously reported spectra is here resolved into two bands for the natural abundance NO adduct (trace A), one located at 434 cm^{-1} and the other at 450 cm^{-1}. The line at 450 cm^{-1} exhibits behavior similar to that of the 449-cm^{-1} band of the $(Mb)Fe^{II}$–NO upon isotopic substitution. The isotopic sensitivity can be more clearly visualized as a positive and a negative peak in the difference spectrum (trace E). It is found that the spectral feature that is assignable to ν(Fe–NO) consists of two bands, a major peak at 546 cm^{-1} and a shoulder. Close examination of the spectra reveals the shoulder disappears in trace B and trace D, while the main band shifts 2 to 3 cm^{-1}. For the $^{14}N^{18}O$ adduct, the shoulder appears again, and the main band moves back. When the band at 546 cm^{-1} is canceled out by subtracting trace D from trace A, as shown in the difference spectrum (trace E), a band at 555 cm^{-1} stands out and a negative peak at 533 cm^{-1} appears. Thus, the simultaneous observation of two isotope-sensitive modes in the low-frequency region is not unique to derivatives of cytochrome P450cam.

(35) Walters, M. A.; Spiro, T. G. *Biochemistry* **1982**, *21*, 6989–6995.
(36) Crull, G. B.; Nardo, J. V.; Dawson, J. H. *FEBS Lett.* **1989**, *254*, 39–42.
(37) Hoffmann, R.; Chen, M. M.-L.; Thorn, D. L. *Inorg. Chem.* **1977**, *16*, 503–511.

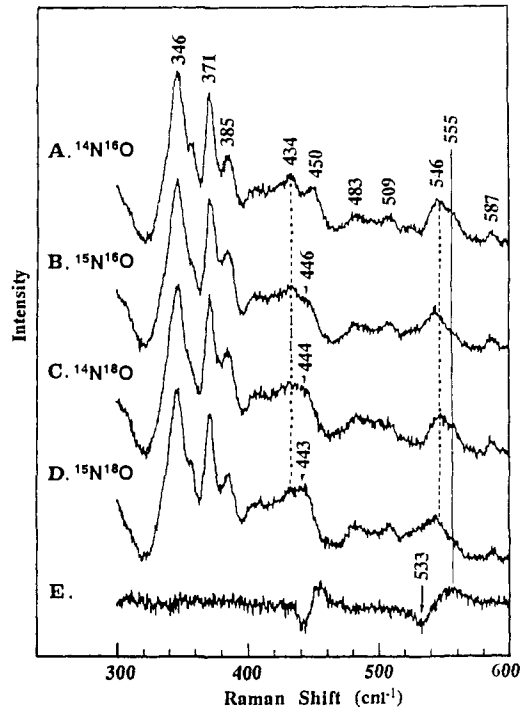

Figure 7. Low-frequency resonance Raman spectra (406.7-nm excitation) of the isotopomeric nitric oxide adduct of ferrous hemoglobin. The concentration of hemoglobin was about 200 μM in 20 mM potassium phosphate buffer at pH 7.0.

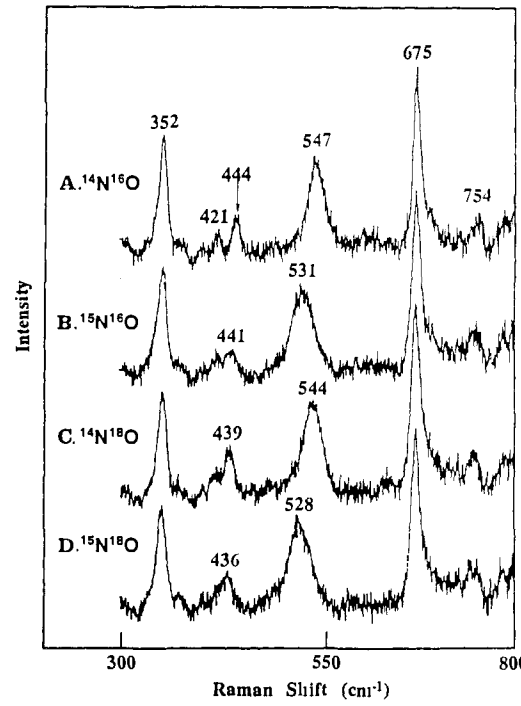

Figure 8. Low-frequency resonance Raman spectra (441.6-nm excitation) of the isotopomeric nitric oxide adduct of substrate-free ferrous cytochrome P450cam. The concentration of the enzyme was 100 μM in 50 mM MOPS buffer (pH 7.4).

Table II. Summary of Fe–NO Vibrational Data (cm^{-1}) of the Nitric Oxide Adducts of Ferrous and Ferric Cytochrome P450cam in the Presence of Various Substrates

	Fe^{II}–NO[a]		Fe^{III}–NO[a]	
substrate	ν(Fe–NO)	δ(FeNO)	ν(Fe–NO)	δ(FeNO)
adamantanone	554 (15, 2, 16)	446 (4, 6, 9)	520 (3)	542 (14)
camphor	553 (13, 2, 14)	445 (2, 6, 9)	522 (2)	546 (13)
norcamphor	545 (17, 1, 16)	441 (3, 4, 7)	524 (3)	
substrate free	547 (16, 3, 19)	444 (3, 5, 8)	528 (4)	

[a] The numerical value in parentheses is the isotopic shift of nitric oxide in the order of $^{15}N^{16}O$, $^{14}N^{18}O$, and $^{15}N^{18}O$.

D. Effect of Substrate Structure on the Low-Frequency Vibrational Modes of the Fe^{II}–NO Fragment in Cytochrome P450cam. Figure 8 shows the RR spectra (441.6-nm excitation) of the isotopic nitric oxide adducts of ferrous cytochrome P450cam in the absence of substrate. The Fe–NO vibrational frequencies of cytochrome P450cam in the presence of various substrate analogues are summarized in Table II. It is immediately apparent that the ν(Fe–NO) and δ(Fe–N–O) modes are sensitive to substrate replacement while the isotopic shift patterns of these two modes are preserved. Correspondingly, bands that exhibit the "zigzag" isotopic shift pattern are assigned to the Fe–NO stretching, while those yielding a monotonous downshift are assigned to the Fe–N–O bending. It is of particular interest to point out here that the wavenumber of the ν(Fe–NO) mode of the norcamphor-bound enzyme is significantly different from those of the adamantanone- and camphor-bound proteins, but essentially the same as that of the substrate-free enzyme. This outcome is in contrast to the results obtained for the RR spectra of the CO adducts[10] and the NO derivatives of ferric cytochrome P450cam,[9] indicating that norcamphor does not exert steric pressure on the ferrous Fe^{II}–NO linkage, even though it is present in the active site.

The effect of camphor binding on the structural change of heme active site in cytochrome P450cam has been studied previously from the viewpoint of both substrate and the bound ligands by several spectroscopic methods. An early infrared study detected distinctly different C–O stretching vibrational frequencies for the carbon monoxide adduct of the substrate-free (1963 cm^{-1}) and camphor-bound (1940 cm^{-1}) ferrous enzyme.[27] In addition, the low-frequency ν(Fe–CO) mode was observed to shift from 481 to 464 cm^{-1} upon the removal of substrate from camphor–CO–ferrous enzyme ternary adduct by recent RR spectral measurement.[10] The observed frequency shifts of both the ν(C–O) and ν(Fe–CO) modes were interpreted as an indication of a bent Fe–C–O structure, presumably resulting from the steric strain imposed by the bound camphor. However, a bent structure for the FeCO fragment was considered very unlikely by Li and Spiro,[34] based on the analysis of the available infrared and RR data on many CO adducts of heme proteins and iron porphyrins. Instead, a tilted (relative to heme plane) distortion coordinate is apparently more plausible.

We recently invesigated the effect of substrate structure on the iron–ligand vibrations in the nitric oxide adduct of ferric cytochrome P450cam and observed an opposite frequency shift for the ν(Fe–NO) mode.[9] Specifically, ν(Fe–NO) vibration is moved from 528 to 522 cm^{-1} upon the binding of camphor to the substrate-free enzyme derivative, the proximal ν(Fe–S) mode being simultaneouslky shifted from 348 to 357 cm^{-1}. In addition, the δ(FeNO) bending mode was enhanced only in the presence of camphor and adamantanone. On the basis of the consideration of both the electronic and the kinematic effect of distortion of the FeNO unit, the vibrational data were interpreted to indicate that the linear, substrate-free derivative is converted to a slightly bent configuration in the presence of substrates.

Additional evidence for a perturbed iron–ligand structure in the camphor-bound adduct comes from a ^{15}N NMR study on the low-spin cyanide complex of cytochrome P450cam.[11] The hyperfine-shifted ^{15}N NMR resonance was detected at 433 and 500 ppm for the substrate-free and camphor-bound adducts, respectively. The result suggests that camphor binding increases unpaired spin density at the cyanide nitrogen atom, presumably by forcing the Fe–C–N linkage to bend or to tilt away from the normal of the heme plane. In another study, the binding of camphor to the active site of cytochrome P450cam in the carbon monoxide adduct was complementarily confirmed by a ^{19}F NMR measurement of the bound 9-fluorocamphor and 5,5-difluorocamphor.[36]

In summary, spectroscopic studies of the adducts with various diatomic ligands (CO, NO, and CN^-) have firmly established that

the intrinsically linear FeXY fragment experiences structural distortion so as to accommodate substrates. This is clearly seen in the crystal structure of the carbon monoxide adduct of camphor-bound cytochrome P450cam, in which camphor is moved away from the CO molecule by about 0.8 Å and FeCO linkage is bent (168°).

E. Relevance to the Issue of Metabolic Regioselectivity. Cytochrome P450cam exhibits remarkable regiospecificity, metabolizing camphor exclusively to the 5-*exo*-hydroxycamphor, both in vivo and in the reconstituted system. On the other hand, Atkins and Sligar[8d] have recently shown that in the cytochrome P450cam catalyzed hydroxylation of norcamphor (a substrate analogue lacking the three methyl groups) at least three products were obtained and that the oxidase activity (gauged by the 4-electron reduction of atmospheric dioxygen to water) of the system is raised. The present RR study of the ferrous NO adducts with various substrates is thus of particular interest inasmuch as this derivative, like the physiologically relevant O_2 adduct, adopts an inherently bent configuration whereas those previously studied (ferrous–CO and ferric–NO) are intrinsically linear. Indeed, the present results, which document the lack of an effect of norcamphor upon the vibrational frequencies of the bound Fe^{II}–NO fragment, are thus consistent with the enzymatic studies by Atkins and Sligar, which imply that even partial relaxation of the steric constraints can result in a loss of metabolic specificity.

Acknowledgment. This work was supported by a grant from the National Institutes of Health (DK35153). The authors are sincerely grateful to Professor S. Sligar of the University of Illinois at Urbana—Champaign for the supply of *P. putida* cell paste.

Registry No. Adamantanone, 700-58-3; camphor, 76-22-2; norcamphor, 497-38-1.

Geometry of the Cyclopropane-1,1-dicarboxylic Acid Molecule at 5 K

J. Krzystek and Alvin L. Kwiram*

Contribution from the Department of Chemistry, University of Washington, Seattle, Washington 98195. *Received April 18, 1991*

Abstract: In our continuing study of the conformation of small cyclic organic molecules at low temperatures we investigated single crystals of deuterated cyclopropane-1,1-dicarboxylic acid by ENDOR-detected nuclear magnetic resonance (EDNMR) at 5 K. The quadrupole tensors of the ring-bonded deuterons (e^2qQ/h = 185 kHz, η = 0.06) allow us to draw conclusions about the geometry of the ring itself. The D–C–D bond angle in both methylene groups (116°) and the angle between the methylene planes (132°) are discussed in terms of carbon hybridization and interactions between hydrogen atoms. The quadrupole splitting parameters of the carboxyl-bonded deuterons (e^2qQ/h = 160 kHz, η = 0.18) yield information on the length of hydrogen bonds. Since e^2qQ is essentially identical for both the intra- and intermolecular bonds, it appears that the bonds have approximately the same length of 1.63 Å. By contrast, the X-ray diffraction results at room temperature show a significant difference in hydrogen bond length defined as the O···H distance (1.63 versus 1.75 Å). This suggests that the intermolecular hydrogen bond has become considerably shorter at low temperature.

Introduction

The geometry of small cyclic molecules like cyclopropane or cyclobutane has been of considerable interest for years. Specifically, the objects of particular interest were the angles formed by the C–C bonds. The bond angles are of course much smaller than those typical of conventionally defined carbon hybridizations, and the molecules are apparently "strained". And yet both molecules mentioned, and many of their derivatives, are completely stable.

Many models have been invoked to account for this paradox (see reviews[1,2]). One of the most successful descriptions is the "bent bond" model devised by Coulson and Moffitt.[3] This model uses three sets of methane-like sp^3 carbon orbitals and constructs from then the alicyclic ring. The direction of maximum overlap in these orbitals in the cyclopropane model lies outside the line connecting the two carbon atoms, thereby justifying the name.

An alternative model of Walsh[4] introduced the concept of a rehybridization in cyclopropane. According to this model, the actual hybridization of the carbon orbitals pointing toward the hydrogen atoms is closer to sp^2 rather than the expected sp^3, which means that the s character is larger than the 0.25 value characteristic for sp^3 hybridization. To compensate for this shift, the s character of the orbitals participating in the C–C bonds must be smaller than 0.25.[1] These predictions were supported by ^{13}C NMR experiments, where the C–C and C–H coupling constants, J, yielded approximately 0.33 s character in the C–H bonds[5] and 0.17 s character in the C–C bonds.[6] In the case of cyclopropane one can thus speak of two sp^2 (0.33 s character) and two "sp^5" (0.17 s character) orbitals for each carbon atom.[1,7] The rehybridization has a direct effect on the spatial character of the orbitals. In fact, various experimental methods, directly or indirectly measuring the C–H bond lengths and H–C–H angles in cyclopropane and its derivatives, have confirmed the NMR data regarding the orbitals involved in C–H bonds. Information on these parameters is, however, far from being complete.

For this and other reasons we embarked on an investigation of cyclopropane-1,1-dicarboxylic acid (CPDA), using the method of ENDOR-detected nuclear magnetic resonance (EDNMR).

(1) Greenberg, A.; Liebman, J. F. *Strained Organic Molecules*; Academic Press: New York, 1978.
(2) Newton, M. D. In *Applications of Electronic Structure Theory*; Schaefer, H. F., Ed.; Plenum Press: New York, 1977.
(3) Coulson, C. A.; Moffitt, W. E. *Philos. Mag.* **1949**, *40*, 1–35.
(4) Walsh, A. D. *Trans. Faraday Soc.* **1949**, *45*, 179–190.
(5) Muller, N.; Pritchard, D. E. *J. Chem. Phys.* **1959**, *31*, 768–771.
(6) Weigert, F. J.; Roberts, J. D. *J. Am. Chem. Soc.* **1967**, *89*, 5962–5963.
(7) Schleyer, P. v. R. *NATO ASI Series, Ser. C (Substituent Effects in Radical Chemistry)* **1986**, *189*, 69–81.

0002-7863/91/1513-9766$02.50/0